Journal of Materials Chemistry B

Accepted Manuscript

This article can be cited before page numbers have been issued, to do this please use: L. Qiao, H. Nie, Y. Wu, F. Xin, C. Gao, J. Jing and X. Zhang, *J. Mater. Chem. B*, 2016, DOI: 10.1039/C6TB02774A.

ROYAL SOCIETY OF CHEMISTRY

rsc.li/materials-b

View Article Online
DOI: 10.1039/C6TB02774A

An ultrafast responsive BODIPY-based fluorescent probe for the detection of endogenous hypochlorite in live cells

Liang Qiao, Hailiang Nie, Yulong Wu, Fangyun Xin, Congcong Gao, Jing Jing* and Xiaoling Zhang*

Key Laboratory of Cluster Science of Ministry of Education, Beijing Key Laboratory of Photoelectronic/Electrophotonic Conversion Materials, School of Chemistry and Chemical Engineering, Beijing Institute of Technology, Beijing 100081, P. R. China.
E-mail: zhangxl@bit.edu.cn (X. Zhang); Tel./fax: +86-010-88875298.
E-mail: hellojane@bit.edu.cn (J. Jing); Tel./fax: +86-010-81381351.

Abstract

Hypochlorite plays a significant role in various physiological and pathological processes, however, its role is still less clear than other reactive oxygen species. Herein, we reported an ultrafast responsive (<0.2s) and highly selective probe B-Ts for hypochlorite with high sensitivity and a detection limit as low as 7.5nM. The probe was compatible with a wide pH range of 4-13. More importantly, experiments in live cells showed that the probe could penetrate cell membrane easily and was capable of imaging endogenous and exogenous hypochlorite specifically with fast response.

1. Introduction

Reactive oxygen species (ROS) are unavoidable products of metabolism and once were thought harmful to organisms. However, advances in research have shown that ROS are a double-edged sword, being capable of mediating both prevention and promotion of diseases. [1,2] Hypochlorous acid (HClO), as a kind of ROS, mainly originates from the reaction of H_2O_2 and Cl^- catalysed by myeloperoxidase (MPO).[3,4] With a pKa value of 7.53, it exists as a mixture of the undissociated acid and the hypochlorite ion(ClO^-) at physiological pH.[5] If generated under regulation, it helps to maintain normal physiological activities and plays a pivotal role in the innate immune defence against pathogens. However, disorder of MPO or other reasons could cause abnormal production of hypochlorite, leading to oxidation of biomolecules which results in tissue damage and contributes to the progression of numerous human diseases, such as atherosclerosis, cardiovascular diseases, rheumatoid arthritis and even cancer.[4,6-12]

The basal $HClO/ClO^-$ level in cells is quite low. It is reported that the average $HClO/ClO^-$ generation from neutrophils is 0.47nmol/min per 10^6 cells.[13] Recently, Peng *et. al.* designed and applied a boron dipyrromethene (BODIPY)-based probe to successfully estimate that the average basal $HClO/ClO^-$ concentrations in MCF-7 and HeLa cells are *ca.* 9.45 and 8.23nM, respectively.[14] Yu *et. al.* further estimated the average basal $HClO/ClO^-$ concentrations in the mitochondria of HeLa and A549 cells to be 46.3 nM and 49.7nM, respectively, using the ratiometric fluorescent probe they designed.[15] Besides, $HClO/ClO^-$ is very reactive and tends to be short-lived in cells.[5] Great progress has been made to design various probes for hypochlorite, however, problems still exist, such as slow response time, low quantum yield. Considering all the above factors, the design of fast responsive and highly sensitive probe is still highly desired.

Fluorescence sensing methods have attracted increasing attention due to the advantages of high sensitivity and feasibility of real-time detection of analytes in solution and live cells. Probes based on fluorophores, nanomaterials as well as polymers have been designed to detect various analytes.[16-18] Unbridged C=N moiety anchored to a fluorophore practically undergo isomerization when in excited state. This isomerization process exhausts the excited energy and renders the fluorophore nonfluorescent. Blockage or removal of this process promises to recover the fluorescence. There has been some probes designed based on this strategy for the detection of various analytes, such as metal ions[19,20] and hypochlorite[6,10,12,21]. $HClO/ClO^-$ can specifically oxidize the C=N moiety into aldehyde group[22-25], carboxylic group[12] or nitrile oxide[6,10,26], consequently, the isomerization process is removed and the fluorophore turns fluorescent again.

Herein, we reported the synthesis, characterizations and application of a novel BODIPY-based probe B-Ts for HClO/ClO^- detection. The probe was conveniently synthesized by condensation of aldehyde group of BODIPY with the hydrazide group of tosylhydrazide to form a C=N moiety. The as-prepared probe can selectively detect hypochlorite with ultrafast response and a robust fluorescence enhancement as well as a clear change of colour from pink to green that can be observed by naked eyes. The limit of detection can be as low as 7.5nM. Moreover, the probe has been successfully utilized to image endogenous and exogenous hypochlorite in live cells.

2. Experimental

2.1 Materials and Instruments

All the reagents were at least of analytical grade and were used directly without further purification. A 5mM solution of probe B-Ts was prepared in ethanol and stored in a refrigerator for use. All ions were added in the form of sodium or chloride salts. Hypochlorite was prepared from commercial sodium hypochlorite solution purchased from Alfa Aesar, and the concentration was determined by measuring the absorbance of the diluted solution in pH=12 NaOH solution at 294nm, where the absorptivity is 350 M^{-1} cm^{-1}. The UV-vis spectra were taken on TU-1901 spectrometer (Beijing Persee General Co., Ltd.) and fluorescence spectra were recorded using a Hitachi F7000 spectrometer with a 10mm quartz cuvette and slit widths of 2.5 nm. The ^{1}H-NMR (400 MHz) and ^{13}C-NMR(125 MHz) spectra were measured on Bruker Ascend NMR spectrometer. Chemical shifts were reported in ppm with TMS as internal reference. Electrospray ionization (ESI) mass spectra were acquired with a Bruker Apex IV FTMS instrument. pH measurements were made with a Mettelor-Toledo FE28 pH-meter. Confocal imaging was performed on Olympus FV1000-LX81. Slight pH variations in the solutions were achieved by adding the minimum volumes of NaOH or HCl (1 M). The water used throughout the experiments was deionized. All measurements were conducted at least in triplicate.

2.2 Synthesis and characterizations of the probe

Synthesis of the probe B-Ts is shown in Scheme 1. To a solution of B-CHO (0.7044g, 2mmol) in methanol was added dropwise methanol solution of tosylhydrazide (0.3911g, 2.1mmol). The system was stirred at r.t. for 8h. Then the solvents were evaporated and the crude product was further separated using column chromatography (PE: EA=4:1, v/v) to yield a red solid. ^{1}H NMR (400 MHz, $CDCl_3$, 25 °C) δ 7.79 (d, *J* = 8.3 Hz, 2H), 7.73 (s, 1H), 7.55 (s, 1H), 7.52- 7.47 (m, 3H), 7.28 (d, *J* = 8.0 Hz, 2H), 7.26- 7.21 (m, 2H), 6.05 (s, 1H), 2.60 (d, *J* = 20.9 Hz, 6H), 2.41 (s, 3H), 1.39 (d, *J* = 12.0 Hz, 6H); ^{13}C NMR (176 MHz, $CDCl_3$, 25 °C) δ 158.42, 154.43, 145.31, 144.19, 143.24, 142.41, 140.19, 135.05, 134.51, 132.62, 130.26, 129.57, 129.29, 129.26, 128.02, 127.82, 122.64, 122.49, 21.58, 14.81, 14.61, 14.05, 12.03. HR ESI-MS calcd for $C_{27}H_{28}BF_2N_4S^+$ [M+H^+]: 521.1989, found 521.1988.

2.3 Determination of quantum yield

The quantum yield of B-CHO and B-Ts was measured in ethanol with fluorescein in 0.1 M NaOH solution as the standard. The absorbance of the solutions should be in the range of 0-0.1 to minimize the re-absorption effect. The excitation wavelength was set at 470nm, and the emission range was 480-650nm with the slit widths set at 2.5 nm. The quantum yield was calculated using the following equation:

$$\Phi=\Phi_S\times(F/F_S)\times(A_S/A)\times(n^2/n_s^2)=\Phi_S\times(G/G_S)\times(n^2/n_s^2)$$

where Φ is the fluorescence quantum yield, A is the absorbance at the excitation wavelength, F is the area under the corrected emission curve, G is the gradient of the curve of integrated intensity against absorbance at λ=470nm and n is the refractive index of the solvents used. Subscript S refers to the standard. For 0.1 M NaOH, we used the wavelength-dependent refractive index of water. Also for ethanol, a wavelength-dependent refractive index was used.

2.4 Determination of limit of detection

The detection limit was calculated based on the fluorescence titration curve of B-Ts in the presence of ClO^-. The fluorescence intensity of B-Ts was measured twenty times and the standard deviation of blank

View Article Online
DOI: 10.1039/C6TB02774A

measurements was achieved. The detection limit was calculated using the following equation:

$$\text{Detection limit} = 3\sigma/k$$

where σ is the standard deviation of blank measurements, k is the slop of the fluorescence intensity versus ClO^- concentrations.

2.5 MTT assay

RAW264.7 cells/HeLa cells of P2 generation were seeded into 96-well plates at a density of 5×10^3 cells per well in culture media (DMEM) in an atmosphere of 5% CO_2 and 95% air at 37ºC and were allowed to grow overnight. The culture media was replaced and 0.5, 1, 5, 10, 15, 20, 40μg/L (final concentration) were added respectively. The cells were incubated at 37 ℃ in an atmosphere of 5% CO_2 and 95% air for 24h. Subsequently, 10μL 3-(4,5-dimethylthiazol-2-yl)-2,5-diphenyltetrazolium bromide (MTT, 5mg/mL) was added and the cells were further cultured for another 3h, respectively. Finally, 100μL DMSO was added to each well and the absorbance at 570nm was measured using microplate reader (Bio-rad 680).

2.6 Cell imaging

HeLa and RAW264.7 macrophages were maintained in DMEM supplemented with 10% heat-inactivated fetal bovine serum (Gibco) and 1% penicillin/streptomycin at 37 ℃ with 5% CO_2. The growth medium was renewed every two to three days. Cells were grown to 80% confluence prior to experiment. B-Ts (1 μM) was added (the concentration of DMSO was maintained to be less than 0.2 %) and cells were further incubated for 5 min, followed by washing twice with phosphate-buffered saline (PBS). The fluorescence imaging was performed with OLYMPUS FV-1000 inverted fluorescence microscope with 100× objective lens. Under the confocal fluorescence microscope, B-Ts was excited at 488 nm and emission was collected at 490-560 nm. For the ClO^--blocking experiment, HeLa cells were pretreated with GSH (10mM) for 15min, and then treated with B-Ts (1μM) for 5 min. For the detection of exogenous ClO^-, HeLa/RAW264.7cells were incubated with B-Ts (1μM, 5 min) and then ClO^- (5μM) was added. For the detection of endogenously produced ClO^-, RAW264.7 cells were pretreated with LPS (1μg/mL) for 24h and PMA (1μg/mL) for 0.5 h before they were incubated with B-Ts (1μM) for 5 min.

3 Results and discussion

3.1 Photophysical properties of B-Ts and B-CHO

While the B-CHO ethanol solution is green and shows strong fluorescence, the as-prepared probe looks pink in dilute solution and becomes nonfluorescent, as can be seen in the insets of Fig.1. The detailed photophysical properties data of B-CHO and B-Ts are given in Table 1.

3.2 Response of B-Ts toward ClO^-

First, the reaction media was examined to optimize the detection condition. Among various systems tested, a combination of H_2O-EtOH (1:1, v/v) proved most efficient for the sensing process.

Then, the response of B-Ts to ClO^- was examined by UV-vis absorption and fluorescence titration. As seen in Fig. 1a, the absorbance at 523nm decreased with the increasing addition of ClO^- and this value declined to nearly zero at last, proving the almost full conversion of the probe. Meanwhile, a new absorption peak gradually appeared at 493nm and reached its climax in the end. The conversion rate calculated with the maximum absorption (i.e. the initial Abs of B-Ts and final Abs of B-CHO) and corresponding extinction coefficient ε could be as high as 96.73%. In the meantime, an isobestic point gradually showed itself at 505nm. Upon the addition of ClO^-, the colour of the system changed immediately from pink to green, which can be easily observed by the naked eyes.

The fluorescence intensity at 508 nm rose rapidly before reaching the maximum as the amount of ClO^- increased, with a nearly 120-fold increase, as shown in Fig. 1b. The fluorescence intensity reached a plateau after 20μM or more ClO^- was added. In the range of 0 to 15μM, the fluorescence intensity was in good linear relationship (R^2 = 0.99789) with the amount of hypochlorite as shown in Fig. 1c. The limit of detection (LOD) was calculated to be 7.5nM according to the IUPAC criteria (LOD=3σ/k). In comparison, a LOD of such level is satisfactory, considering the number of probes with a LOD lower than 10nM is still scarce.[14,15,21,25,27-29]

The response time of B-Ts toward ClO^- was about 0.2s measured by time scan fluorometry as shown in Fig. 1d. The fluorescence intensity of the system before and after the addition of ClO^- were stable, which indicated that B-Ts and the product were of good stability.

3.3 The effect of pH

The effect of pH was also investigated and the results were depicted in Fig. 2. While the fluorescence intensities of B-Ts under different pH's were weak and almost identical, the fluorescence intensities of the system after the addition of 5 equivalents of ClO^- increased rapidly and significantly, especially in the pH range of 4-13. Few hypochlorite probes with such a wide pH compatibility has been reported in the literature.[14,30-32] More importantly, in the physiological pH range, the fluorescence intensities were almost constant and in the climax, proving that the probe is compatible with biological environment.

3.4 Selectivity of the probe

Selectivity is another important indicator of a probe. Cytosol contains a variety of compounds, therefore ROS, RNS, metal ions and reducing agents that commonly exist in cytosols were tested and the results were shown in Fig. 3. In comparison with ClO^-, no obvious changes in fluorescence intensity were observed when 50 equivalents of various species were added. When ClO^- was added to B-Ts solution containing the competing species, the fluorescence intensity increased significantly, proving that the interferences of the competing species were easily discriminable.

3.5 The detection mechanism

To investigate the detection mechanism of B-Ts toward hypochlorite, the reaction product of B-Ts with ClO^- was purified and characterized by ^1H NMR and HRMS. The ^1H NMR spectrum of the reaction product was identical to that of B-CHO as shown in Fig. 4. HR ESI-MS data for the product (353.1634) matched quite well with the value calculated for $C_{20}H_{20}BF_2N_2O^+$ $[M+H^+]$ =353.1631, M=B-CHO. These all proved that the product was indeed B-CHO. Inspired by the reported mechanisms[21,33-36] and the strong oxidizing power of ClO^-, we speculated that ClO^- reacted with C=N moiety first to form an intermediate, which reacted with H_2O to form the final product, as depicted in Scheme 2.

3.6 MTT assay and cell imaging experiments

MTT assay was conducted to evaluate the cytotoxicity of the probe and the results demonstrated that the probe exhibit low cytotoxicity even at a concentration of up to 15μM (Fig. 5).
Finally, the probe was applied to image hypochlorite in HeLa and RAW264.7 cells. After 5min's incubation of HeLa cells with 1μM B-Ts, the intracellular part of the cells gave green fluorescence, which indicated that our probe was cell membrane permeable. Much stronger green fluorescence could be observed instantly when 5μM ClO^- was added to HeLa cells that were treated with B-Ts. While HeLa cells pretreated with 10mM GSH, which is commonly used as a ClO^- scavenger, for 15min followed by the incubation of B-Ts showed much dimmer fluorescence under comparison. These phenomena indicated that it is hypochlorite that has caused the fluorescence enhancement. Meanwhile, RAW264.7 cells treated with B-Ts showed almost no green fluorescence, which agrees well with the fact that cancers cells, in comparison, are under more severe oxidative stress than normal cells and demonstrated that the probe could distinguish HeLa cells from RAW264.7 cells. RAW264.7 cells that were treated with B-Ts followed by adding ClO^- gave strong green fluorescence. What's more, when incubated with B-Ts, RAW264.7 cells pretreated with LPS for 24h followed by PMA for 30min showed green fluorescence, which meant that our probe was capable of detecting endogenous ClO^-.

4 Conclusion

In summary, a novel BODIPY-based probe B-Ts that can selectively detect ClO^- has been developed by attaching a C=N moiety to the fluorophore. The probe responded to ClO^- rapidly (< 0.2s) with a clear change of color of solution from pink to green and a robust fluorescence enhancement. The LOD can be as low as 7.5 nM and the probe was compatible with a wide range of pH (4-13). What's more, experiments demonstrated that the probe could be utilized for imaging both endogenous and exogenous hypochlorite in live cells. The new probe is expected to be utilized in chemical, biological and environmental applications.

View Article Online
DOI: 10.1039/C6TB02774A

Acknowledgements

We gratefully acknowledge financial support from the National Natural Science Foundation of China (No. 21275018, 21575015, 21505004 and 21203008), Beijing National Laboratory for Molecular Sciences (BNLMS) (20140121), Research Fund for the Doctoral Program of Higher Education of China (RFDP) (No. 20121101110049) and the 111project (B07012) for financial support.

References

1 Seifried, H.; Anderson, D.; Milner, J.; Greenwald, P. *New Developments in Antioxidants Research* **2006**, 1.

2 Khanna, D.; Garg, M. *Handbook on Reactive Oxygen Species (ROS)* **2014**, 197.

3 Yap, Y. W.; Whiteman, M.; Cheung, N. S. *Cellular signalling* **2007**, *19*, 219.

4 Sun, Z.-N.; Liu, F.-Q.; Chen, Y.; Tam, P. K. H.; Yang, D. *Organic Letters* **2008**, *10*, 2171.

5 Klebanoff, S. J. *Journal of leukocyte biology* **2005**, *77*, 598.

6 Emrullahoglu, M.; Ucuncu, M.; Karakus, E. *Chemical communications* **2013**, *49*, 7836.

7 Kim, T. I.; Park, S.; Choi, Y.; Kim, Y. *Chemistry, an Asian journal* **2011**, *6*, 1358.

8 Guo, T.; Cui, L.; Shen, J.; Wang, R.; Zhu, W.; Xu, Y.; Qian, X. *Chemical communications* **2013**, *49*, 1862.

9 Xiao, H.; Xin, K.; Dou, H.; Yin, G.; Quan, Y.; Wang, R. *Chemical communications* **2015**, *51*, 1442.

10 Reja, S. I.; Bhalla, V.; Sharma, A.; Kaur, G.; Kumar, M. *Chemical communications* **2014**, *50*, 11911.

11 Cheng, T.; Zhao, J.; Wang, Z.; An, J.; Xu, Y.; Qian, X.; Liu, G. *Dyes and Pigments* **2016**, *126*, 218.

12 Cheng, G.; Fan, J.; Sun, W.; Sui, K.; Jin, X.; Wang, J.; Peng, X. *The Analyst* **2013**, *138*, 6091.

13 Aratani, Y.; Koyama, H.; Nyui, S.-i.; Suzuki, K.; Kura, F.; Maeda, N. *Infection and immunity* **1999**, *67*, 1828.

14 Zhu, H.; Fan, J.; Wang, J.; Mu, H.; Peng, X. *J Am Chem Soc* **2014**, *136*, 12820.

15 Hou, J. T.; Li, K.; Yang, J.; Yu, K. K.; Liao, Y. X.; Ran, Y. Z.; Liu, Y. H.; Zhou, X. D.; Yu, X. Q. *Chemical communications* **2015**, *51*, 6781.

16 Pu, F.; Ju, E.; Ren, J.; Qu, X. *Advanced Materials* **2014**, *26*, 1111.

17 Li, H.; Zhang, Y.; Wang, L.; Tian, J.; Sun, X. *Chemical communications* **2011**, *47*, 961.

18 Yu, C.; Li, X.; Zeng, F.; Zheng, F.; Wu, S. *Chemical communications* **2013**, *49*, 403.

19 Ye, J.-H.; Xu, J.; Chen, H.; Bai, Y.; Zhang, W.; He, W. *Tetrahedron Letters* **2014**, *55*, 6269.

20 Goh, H.; Kim, M. J.; Saluja, P.; Singh, N.; Jang, D. O. *Tetrahedron Letters* **2012**, *53*, 3900.

21 Wang, B.; Chen, D.; Kambam, S.; Wang, F.; Wang, Y.; Zhang, W.; Yin, J.; Chen, H.; Chen, X. *Dyes and Pigments* **2015**, *120*, 22.

22 Chen, W.-C.; Venkatesan, P.; Wu, S.-P. *New Journal of Chemistry* **2015**, *39*, 6892.

23 Wang, X.; Wang, X.; Feng, Y.; Zhu, M.; Yin, H.; Guo, Q.; Meng, X. *Dalton Trans* **2015**, *44*, 6613.

24 Wu, G.; Zeng, F.; Wu, S. *Analytical Methods* **2013**, *5*, 5589.

25 Guo, B.; Nie, H.; Yang, W.; Tian, Y.; Jing, J.; Zhang, X. *Sensors and Actuators B: Chemical* **2016**, *236*, 459.

26 Li, D.; Feng, Y.; Lin, J.; Chen, M.; Wang, S.; Wang, X.; Sheng, H.; Shao, Z.; Zhu, M.; Meng, X. *Sensors and Actuators B: Chemical* **2016**, *222*, 483.

27 Shen, Y.; Zhang, X.; Huang, X.; Wen, S.; Liu, M.; Deng, Y.; Zhang, Y.; Zhang, C.; Jin, J.; Li, H.; Yao, S. *RSC Advances* **2015**, *5*, 79519.

28 Xiong, K.; Huo, F.; Yin, C.; Chu, Y.; Yang, Y.; Chao, J.; Zheng, A. *Sensors and Actuators B: Chemical* **2016**, *224*, 307.

29 Tang, Z.; Ding, X.-L.; Liu, Y.; Zhao, Z.-M.; Zhao, B.-X. *RSC Advances* **2015**, *5*, 99664.

30 Cheng, G.; Fan, J.; Sun, W.; Sui, K.; Jin, X.; Wang, J.; Peng, X. *The Analyst* **2013**, *138*, 6091.

View Article Online
DOI: 10.1039/C6TB02774A

31 Chen, W.-C.; Venkatesan, P.; Wu, S.-P. *New Journal of Chemistry* **2015**, *39*, 6892.

32 Cheng, X.; Jia, H.; Long, T.; Feng, J.; Qin, J.; Li, Z. *Chemical communications* **2011**, *47*, 11978.

33 Goswami, S.; Maity, S.; Maity, A. C.; Das, A. K. *Sensors and Actuators B: Chemical* **2014**, *204*, 741.

34 Chen, X.; Wang, X.; Wang, S.; Shi, W.; Wang, K.; Ma, H. *Chemistry (Weinheim an der Bergstrasse, Germany)* **2008**, *14*, 4719.

35 Cheng, X.; Jia, H.; Long, T.; Feng, J.; Qin, J.; Li, Z. *Chemical communications* **2011**, *47*, 11978.

36 Wang, Y.; Xia, J.; Han, J.; Bao, X.; Li, Y.; Tang, X.; Ni, L.; Wang, L.; Gao, M. *Talanta* **2016**, *161*, 847.

37 Magde, D.; Wong, R.; Seybold, P. G. *Photochemistry and Photobiology* **2002**, *75*, 327.

View Article Online
DOI: 10.1039/C6TB02774A

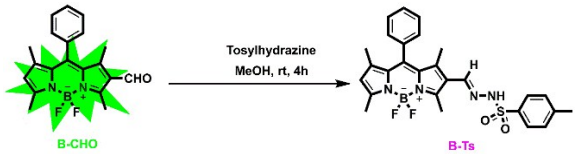

Scheme 1. Synthesis of the probe B-Ts

Table 1. Photophysical properties of B-CHO and B-Ts

Compound	ε/L cm^{-1} mol^{-1} [a]	λ_{Abs}[a]	ϕ[b]	λ_{em}[a]	δ
B-CHO	8.12×10^4	493	0.614	508	15
B-Ts	5.12×10^4	523	0.0272	565	42

a) All the photophysical properties data were acquired in the ethanol solution of corresponding compounds. b) quantum yields were measured with fluorescein in 0.1 M NaOH aqueous solution as standard (ϕ=0.925).[37] δ is the stokes shift.

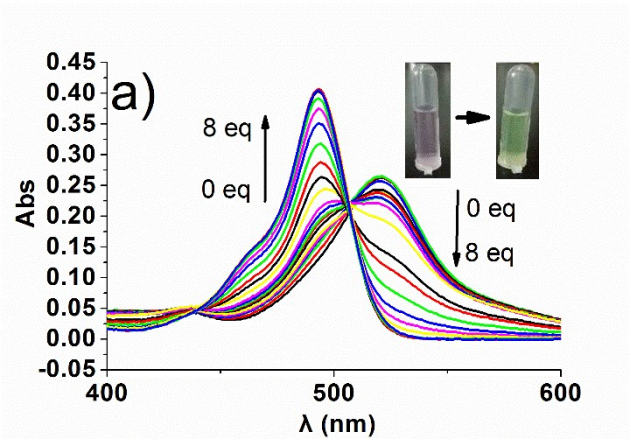

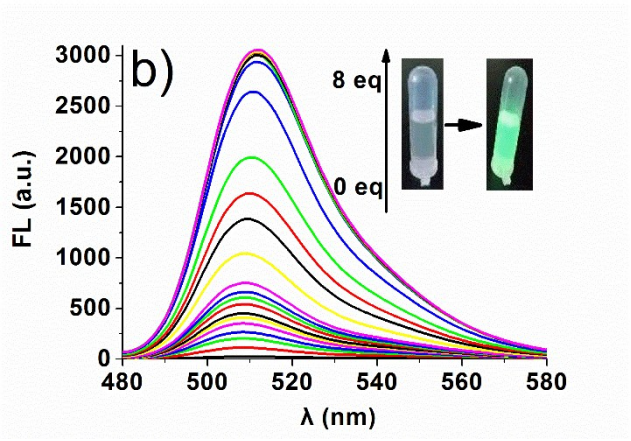

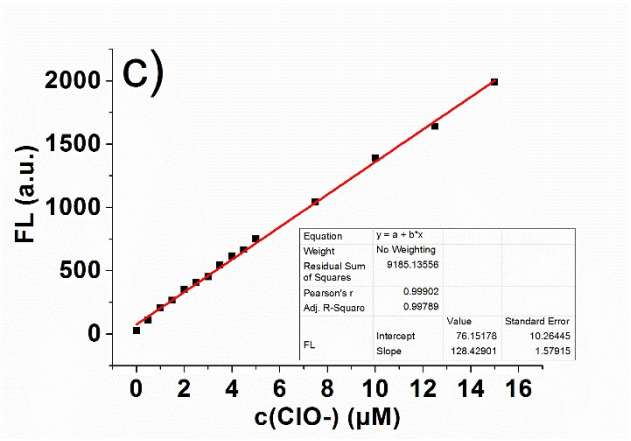

View Article Online
DOI: 10.1039/C6TB02774A

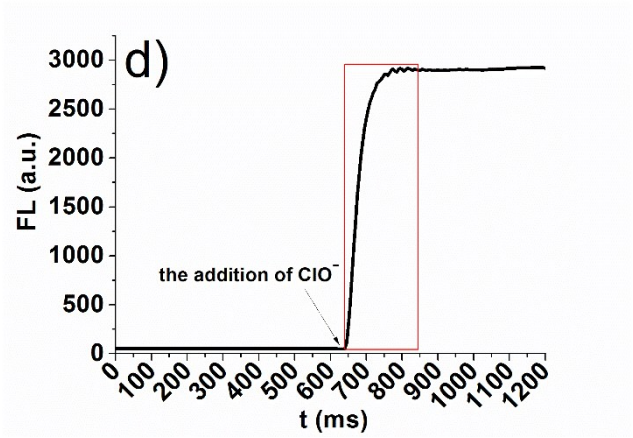

Fig. 1 The change of a) UV-vis absorption and b) fluorescence spectra of 5μM B-Ts in PBS buffer (pH 7.4, 10mM) and EtOH (1:1, v/v) with different equivalents of ClO^- added. Insets: a) photos of B-Ts solution before (left) and after (right) the addition of 5 equivalents of ClO^-, b) photos of B-Ts solution before (left) and after (right) the addition of 5 equivalents of ClO^- under the irradiation of 365nm light. λex=470 nm, slit widths are set at 2.5 nm. c) the linear relationship between fluorescence intensity and ClO^- added in the range of 0-15μM. d) time scan fluorometry of 5μM B-Ts before and after the addition of 5 equivalents of ClO^-, arrow indicates the time when ClO^- was added.

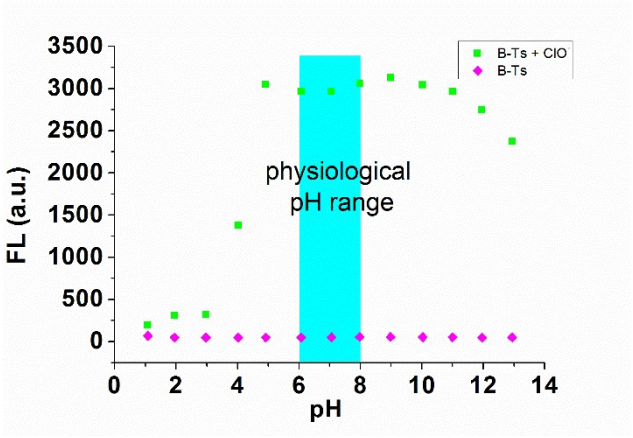

Fig. 2 The fluorescence intensity of 5μM B-Ts at 508 nm in PBS buffer (10mM) and EtOH (1:1, v/v) under different pH (1-13) before (pink squares) or after (green squares) the addition of 5 equivalents of ClO^-.

View Article Online
DOI: 10.1039/C6TB02774A

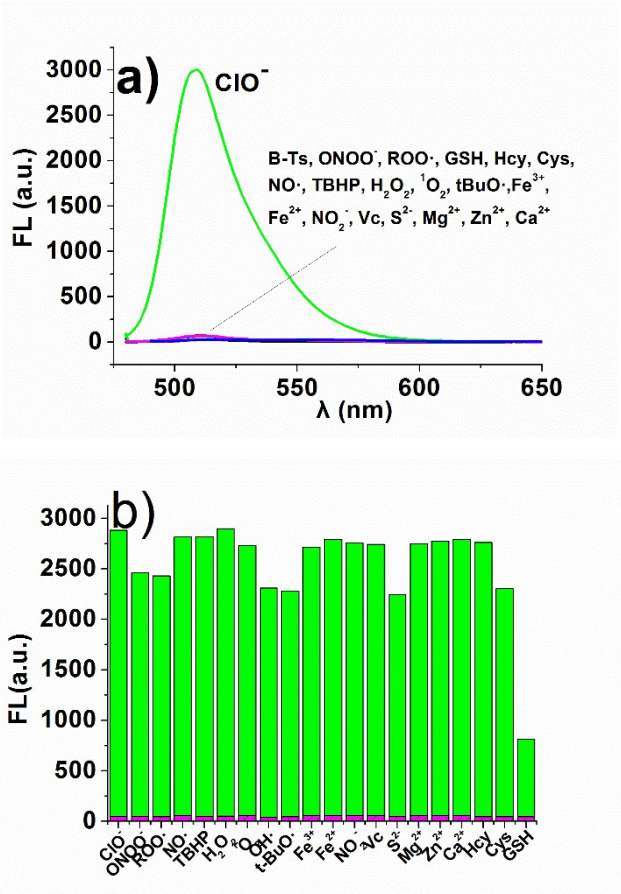

Fig. 3 a) Selectivity of B-Ts probe toward ClO^- against other competing species. Fluorescence intensity of B-Ts solution after 50 equivalents of various species were added while the concentration of GSH, Hcy and Cys were 10mM, 0.01mM and 0.2mM, respectively. b) Competition of various analytes with ClO^- toward B-Ts: pink parts: fluorescence intensity of B-Ts solution in the presence of different equivalents of various species: 10 equivalents of $ONOO^-$, 20 equivalents of ROO·, 50 equivalent of NO·, TBHP, H_2O_2, $^1O_2$, OH·, t-BuO·, Fe^{3+}, Fe^{2+}, NO_2^-, Vc, Mg^{2+}, Zn^{2+}, Ca^{2+}, 8 equivalents of S^{2-}, 2000 equivalents (10mM) of GSH, 40 equivalents (0.2mM) of Cys and 2 equivalents (0.01mM) of Hcy. Green parts: fluorescence intensity of the above solutions after ClO^- was added.

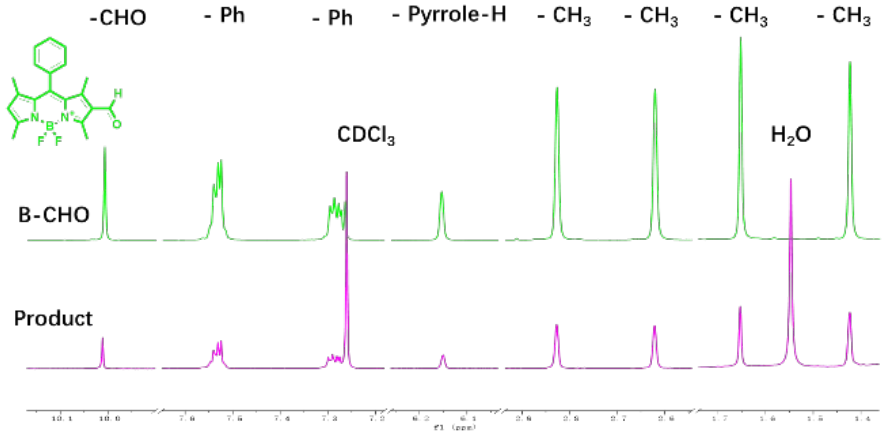

Fig. 4 Comparison of parts of the ^1H NMR spectra of B-CHO (top) and the reaction product of B-Ts with ClO^- (below).

View Article Online
DOI: 10.1039/C6TB02774A

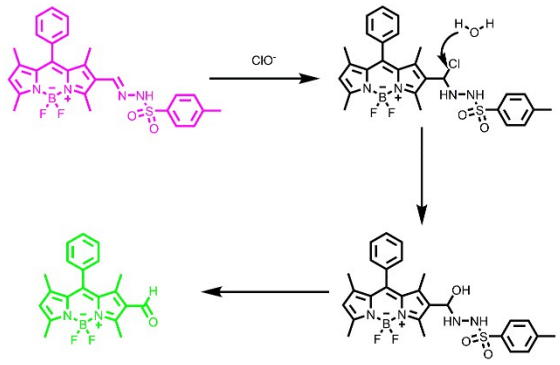

Scheme. 2 Proposed reaction mechanism of B-Ts with ClO^-

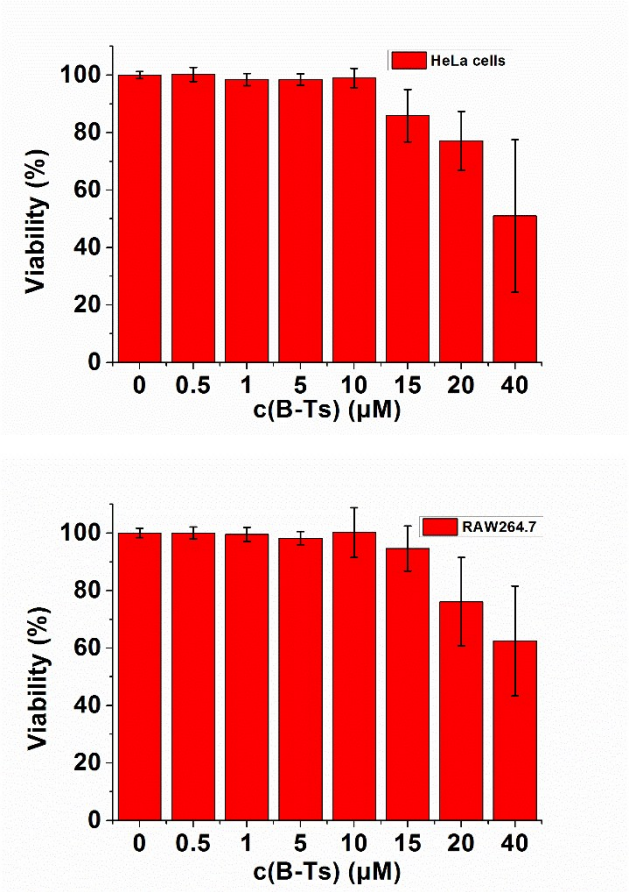

Fig. 5 The cytotoxicity of different concentrations of B-Ts (0.5, 1, 5, 10, 15, 20 and 40μmol/L) in HeLa (a) and RAW264.7 (b) cells.

View Article Online
DOI: 10.1039/C6TB02774A

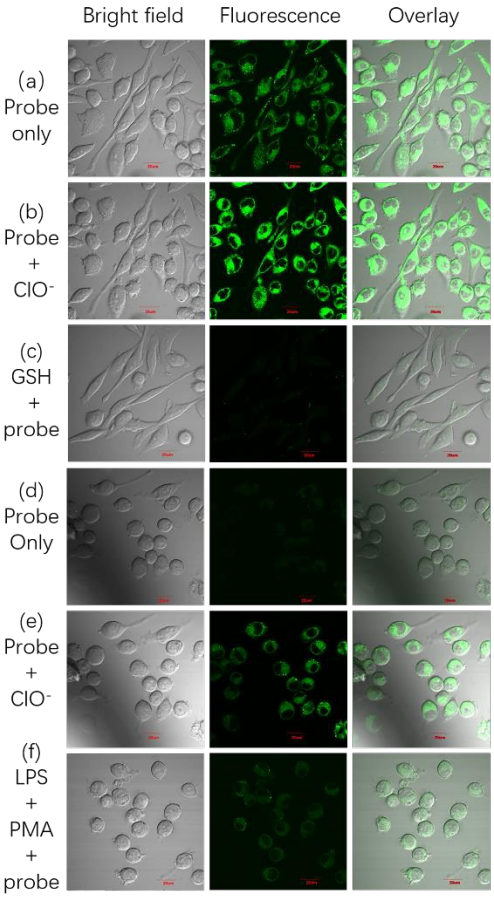

Fig. 6 Bright field (left), fluorescence (middle) and overlay (right) images of (a) HeLa cells treated with 1μM B-Ts only, (b) HeLa cells treated with 1μM B-Ts followed by the addition of 5μM ClO^-, (c) HeLa cells pretreated with 10mM GSH and incubated with 1μM B-Ts; (d) RAW264.7 cells treated with 1μM B-Ts only, (e) RAW264.7 cells treated with 1μM B-Ts followed by the addition of 5μM ClO^-, (f) RAW264.7 cells pretreated with 1μg/mL LPS for 24h and 1μg/mL PMA for 30min before incubated with 1μM B-Ts, respectively.

View Article Online
DOI: 10.1039/C6TB02774A

An ultrafast responsive BODIPY-based fluorescent probe for the detection of endogenous hypochlorite in live cells

Liang Qiao, [a] Hai-Liang Nie, [a] Yu-Long Wu, [a] Fang-Yun Xin, [a] Cong-Cong Gao, [a] Jing Jing, * [a] and Xiao-Ling Zhang*[a]

Key laboratory of Cluster Science of Ministry of Education

Beijing Key Laboratory of Photoelectronic / Electrophotonic Conversion Materials
School of Chemistry and Chemical Engineering
Beijing Institute of Technology

5 South Zhongguancun Street, Beijing 100081, P. R. China.

E-mail: zhangxl@bit.edu.cn, hellojane@bit.edu.cn

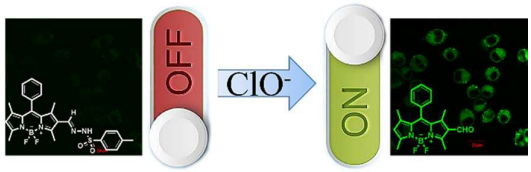

An ultrafast responsive BODIPY-based fluorescent probe was synthesized that can selectively detect endogenous hypochlorite in live cells.